Received: *April 23, 2001*, Accepted: *May 21, 2001*

QCD analysis of D-parameter in near-to-planar three-jet events

Andrea Banfi and Giuseppe Marchesini

Dipartimento di Fisica, Università di Milano–Bicocca and INFN
Sezione di Milano, Italy
E-mail: Andrea.Banfi@mib.infn.it, giuseppe.marchesini@mib.infn.it

Yuri L. Dokshitzer*

LPT, Université de Paris XI, Centre d'Orsay, France
E-mail: Yuri.Dokshitzer@th.u-psud.fr

Giulia Zanderighi

Dipartimento di Fisica Nucleare e Teorica
Università di Pavia and INFN
Sezione di Pavia, Italy
E-mail: zanderi@osfmite.mi.infn.it

Abstract: We present the QCD analysis of D-parameter distribution in near-to-planar 3-jet e^+e^- annihilation events. We derive the all-order resummed perturbative prediction and the leading power suppressed non-perturbative corrections both to the mean value and the distribution. Here non-perturbative corrections are larger than in 2-jet shape observables, so that higher order non-perturbative effects could be relevant. Experimental data (not yet available) are needed in order to cast light on this important point. The technique we develop aims at improving the accuracy of the theoretical description of multi-jet ensembles, in particular in hadron-hadron collisions.

Keywords: QCD, Jets, LEP HERA and SLC Physics, Non-perturbative Effects.

*on leave from PNPI, Gatchina, St. Petersburg, 188350, Russia

JHEP05(2001)040

Contents

1. Introduction

The analysis of event shape distributions in e^+e^- has provided various tests of QCD [1] and measurements of the running coupling [2]. The shape observables which have been most intensively studied and tested are: thrust T, C-parameter, jet mass M^2 and broadening B. Their distributions are collinear and infrared safe (CIS) and therefore can be computed order-by-order in perturbation (PT) theory.

Specially interesting is the region of two narrow jets ($1-T, C, M^2/Q^2, B \ll 1$), where the PT expansion needs to be resummed so that the QCD structure is most intensively probed. The available PT results [3] for these typical 2-jet observables[2] involve all-order resummation of double- (DL) and single-logarithmic (SL) contributions and matching of the approximate resummed expressions with the exact second order matrix elements.

To make quantitative predictions one needs to go beyond PT calculations and to take into account the $1/Q$-suppressed power corrections arising from the interaction in the confinement region. It has been proposed [4] that these non-perturbative (NP) corrections can be estimated by extrapolating the running coupling into the large distance region. A systematic method for this extrapolation is provided by the dispersive approach [5]. The leading NP corrections to the shape distributions involve a single parameter, usually denoted by α_0, which is given by the integral of the QCD coupling over the region of small momenta $k \leq \mu_I$ (with the infrared scale μ_I conventionally chosen to be $\mu_I = 2\,\mathrm{GeV}$). They have been computed at two-loop level to take into account effects of non-inclusiveness of jet observables [6]. Such a procedure for computing the $1/Q$-power corrections is consistent with the data and the NP parameter α_0 has been measured and appears to be universal with a reasonable accuracy [1].

We have recently studied the distribution in the thrust minor T_m, a CIS shape observable characterising 3-jet events. It starts at order α_s^2 and measures the radiation out of the event plane in e^+e^- annihilation. The event plane is defined by the T and T_M axes, with T_M the thrust major. The most interesting region in which one probes QCD is that of nearly planar 3-jet events, $T_m \ll T_M \sim T$, where PT resummation is needed. The methods developed for the analysis of 2-jet observables $T, C, M^2/Q^2$ and B were extended to the case of T_m in [7].

In this paper we report the analysis of the distribution in another typical 3-jet observable, the D-parameter, which has been introduced in [8]. This is a CIS shape observable which, as T_m, measures the radiation out of the event plane. In the nearly planar 3-jet region ($D \ll 1$), the main difference between D and T_m is that only soft particles at large angles with respect to the event plane, $p_{\mathrm{out}} \sim p_{\mathrm{in}} \propto D \ll 1$, contribute to D, contrary to the T_m case. The fact that energetic hadrons with $p_{\mathrm{in}} \gg p_{\mathrm{out}}$ do contribute to T_m, gives rise, in particular, to additional logarithmic enhancement of the NP contribution from the regions where a small transverse momentum energetic gluon is emitted close to the direction of one of the three jets. This difference is similar to that between B and $T, C, M^2/Q^2$ in 2-jet events [6]: an energetic hadron emitted near the thrust axis contributes to B but does not contribute to the other shape observables.

[2]Sometime these observables are called 3-jet observables since the first contribution involves three particles in the final state. We prefer to call them 2-jet observables since we are interested to the kinematical region in which one particle of the three is soft.

JHEP05(2001)040

Our study is performed with the accuracy necessary to make quantitative predictions. We perform the all-order resummation of DL- and SL-enhanced PT contributions, match it [3] with the exact fixed order matrix element calculation and compute the leading $1/Q$ NP correction at the two-loop order. Actually, the fact that only hadrons at large angles contribute to $D \ll 1$ makes the present analysis significantly simpler than that of T_m.

We find that, as in the T_m case, the structure of the result is quite rich, especially for small D where both the PT and NP components of the D distribution essentially depend on the geometry of the event (the angles between jets). Not only will the analysis of the D distribution provide an alternative measurement of the QCD coupling α_{s}. It gives a powerful tool for accessing genuine confinement hadronisation effects, for extracting the NP parameter α_0 and testing its universality.

The paper is organised as follows. In section 2 we introduce the observable and discuss the characteristic kinematics in the near-to-planar 3-jet region. In section 3 we discuss the resummation procedure. In section 4 we analyse the PT resummation at SL level. In section 5 we analyse the leading NP corrections in terms of the universal parameter α_0. In section 6 we report the final result and discuss the necessary ingredients of the one-loop matching. In section 7 we report the numerical analysis of the distribution and the mean. In section 8 we summarise and discuss the results.

2. The observable

The D parameter is defined as [8]

$$D \equiv 27 \det\theta = 27\lambda_1\lambda_2\lambda_3\,, \qquad \theta_{\alpha\beta} = \frac{1}{\sum_h |\,\vec{p}_h\,|}\sum_h \frac{p_{h\alpha}\,p_{h\beta}}{|\,\vec{p}_h\,|}\,, \tag{2.1}$$

with $\vec{p}_h$ the momentum of the emitted hadron h and $p_{h\alpha}$ its α-component ($\alpha = 1,2,3$). The eigenvalues λ_i satisfy the conditions $0 \le \lambda_i \le 1$ and $\sum_i \lambda_i = 1$. We assume the order $\lambda_3 \le \lambda_2 \le \lambda_1$.

To select near-to-planar events we introduce a lower limit y_c for the 3-jet resolution variable y_3, defined[3] according to the k_T (Durham) algorithm [10]. We study the following normalised integrated distribution

$$\begin{aligned}\Sigma(D, y_c) &= \frac{1}{\sigma(y_c)}\sum_m \int d\sigma_m \Theta(y_3 - y_c)\Theta\left(D - 27\det\theta\right),\\ \sigma(y_c) &= \sum_m \int d\sigma_m \Theta(y_3 - y_c)\,,\end{aligned} \tag{2.2}$$

where $d\sigma_m$ denotes the differential distribution in the m final particles with momenta p_h.

[3] Given the set of all momenta, one defines the "jettiness" variable [9] of any pair p_h and $p_{h'}$ as the quantity $y_{hh'} = 2\,(1-\cos\theta_{hh'})\,\min(E_h^2, E_{h'}^2)/Q^2$. The pair of momenta $p_{\bar h}, p_{\bar h'}$ with the minimum distance $y_3 = y_{\bar h,\bar h'} = \min_{hh'} y_{hh'}$ are substituted with the pseudoparticle (jet) momentum $p_{h''} = p_{\bar h} + p_{\bar h'}$. The procedure is repeated with the new momentum set till only three jets are left. Then the final value of y_3 is defined as the three-jet resolution of the event.

JHEP05(2001)040

We comment here on the fact that we use the variable y_3 to select the 3-jet events (instead of, for instance, the thrust T), which makes it easier to interpret the $1/Q$ power corrections that, as we shall see, are present in the D-distribution. Indeed, the difference between the hadron and parton level values of the thrust variable T is known to be of the order of $1/Q$, while the values of y_3 for hadrons and partons is not affected by $1/Q$ corrections [5]. Therefore, the $1/Q$ contribution to the distribution (2.2) can be looked upon as a genuine NP correction to the variable D. On the contrary, substituting $T < T_c$ for $y_3 > y_c$ in the distribution (2.2), the $1/Q$ correction would have to be shared between D and T.

The region of small D and relatively large y_c (we consider typical values of y_c in the range 0.025–0.1) corresponds to the region

$$\lambda_3 \ll \lambda_2 \lesssim \lambda_1 \,, \qquad T_m \ll T_M \lesssim T \,. \tag{2.3}$$

Here $\lambda_1, \lambda_2, y_3$ and T, T_M are determined by the hard momenta characterising the three jets. The smallest eigenvalue λ_3 and T_m are determined by the out-of-event-plane soft momentum component of the particles around and between the jets (inter- and intra-jet radiation). Taking the plane of the event as the $\{y, z\}$-plane, the dominant contribution to λ_3 in the region (2.3) is given by

$$\lambda_3 \simeq \sum_h \frac{p_{h\,x}^2}{E_h Q} \,. \tag{2.4}$$

Due to the energy factor E_h in the denominator, λ_3 gets the leading contribution from hadrons with $E_h \sim p_{h\,x}$. Instead, the observable T_m

$$T_m = \sum_h \frac{|p_{hx}|}{Q} \,, \tag{2.5}$$

as mentioned in the Introduction, receives contributions from particles with arbitrary large energies, and in particular those that are quasi-collinear with one of the hard jets.

3. Parton process and resummation

Our first aim is to express the distribution $\Sigma(D, y_c)$ in terms of parton processes in the near-to-planar region (2.3). Here the parton events can be treated as 3-jet events generated by a hard quark-antiquark-gluon system accompanied by an ensemble of secondary partons k_i. In this region, the quantities λ_1, λ_2, T, T_M and the 3-jet resolution variable y_3 are determined by the three momenta of the hard quark, antiquark and gluon which we denote by P_1, P_2 and P_3, respectively. Introducing the Born x-invariants (for the Born Kinematics see appendix A)

$$x_a \equiv \frac{2P_a Q}{Q^2} \,, \qquad 2 = x_1 + x_2 + x_3 \,, \tag{3.1}$$

JHEP05(2001)040

we have

$$\lambda_1\,\lambda_2 = \frac{2(1-x_1)(1-x_2)(1-x_3)}{x_1x_2x_3}\,, \qquad y_3 = \frac{x_{\min}(1-x_{\max})}{2-x_{\max}-x_{\min}}\,, \tag{3.2}$$

with

$$x_{\max} = \max\{x_1,x_2,x_3\}\,, \qquad x_{\min} = \min\{x_1,x_2,x_3\}\,. \tag{3.3}$$

At the Born level, all three partons are in the event plane so that $D = \lambda_3 = 0$. With account of secondary partons k_i, radiation out of the event plane is generated and one gets $\lambda_3 > 0$. At the same time, the hard quark, antiquark and gluon momenta acquire recoils and move out of the event plane. In the near-to-planar region (2.3), both the hard parton recoil and the secondary parton momenta can be treated as small (soft).[4] To leading order the smallest eigenvalue λ_3 is given by

$$\lambda_3 = \sum_i \frac{k_{i\,x}^2}{\omega_i Q}\,, \tag{3.4}$$

with $k_{i\,x}$ the out-of-event plane component and ω_i the energy of a secondary soft parton i. Corrections are quadratic in the "soft" parameter $k_x/Q \sim D \ll 1$. In particular, due to the presence of the energy in the denominator, the contributions from the recoiling hard primary partons $q\bar{q}, g$ are of second order ($\mathcal{O}\left(D^2\right)$) and have been neglected in (3.4). The quantities $\lambda_1\lambda_2$ and y_3 are given, to leading order, by (3.2) with corrections linear and quadratic in D, respectively.

3.1 Resummation of soft radiation

The starting point for the parton resummation of the distribution (2.2) is the factorisation of soft emission from the hard parton system. The distribution M_n^2 for the emission of n soft partons from the primary $q\bar{q}, g$ system can be factorised in the form

$$M_n^2\left(P_a, k_1\ldots k_n\right) \simeq M_0^2\left(P_a\right)\cdot S_n\left(P_a, k_1\ldots k_n\right), \tag{3.5}$$

where we have used the fact that the hard parton recoils can be neglected and the actual $q\bar{q}g$ momenta replaced by their Born values P_a. The first factor is the squared first order matrix element giving the Born distribution

$$\frac{d\sigma^{(0)}}{dx_1dx_2} = \frac{C_F\alpha_{\rm s}}{2\pi}\frac{x_1^2+x_2^2}{(1-x_1)(1-x_2)}\,, \qquad \alpha_{\rm s} = \alpha_{\rm s}(Q)\,, \tag{3.6}$$

where, from now on, x_1 and x_2 mark the quark and antiquark invariant energy fractions (or vice versa), and $x_3 = 2 - x_1 - x_2$ is that of the hard gluon.

[4] As we have shown in [7], finite rescaling of the in-plane momenta, due to hard collinear splittings, gets absorbed into the first hard correction to the emission probability of soft gluons, which is then resummed and embodied into the radiator. Bearing this in mind, all hard parton recoils and the secondary parton momenta k_i can be effectively treated as small.

JHEP05(2001)040

The second factor S_n describes the distribution for emitting n soft partons k_i from the hard $q\bar{q}, g$ system. This distribution can also be factorised into the product of independent soft emissions. The structure of this factorisation depends on the required accuracy. Since we aim at SL accuracy, we follow the analysis of [7] in which S_n is factorised at two-loop order.

In the region (2.3), from the factorised expression (3.5), at parton level we can write

$$\begin{aligned} \Sigma(D, y_c) &\simeq \frac{1}{\sigma(y_c)} \int dx_1 dx_2 \, \Theta(y_3 - y_c) \left\{ C(\alpha_s) \cdot \frac{d\sigma^{(0)}}{dx_1 dx_2} \cdot S(D, x_1, x_2) \right\}, \\ \sigma(y_c) &\simeq \int dx_1 dx_2 \, \Theta(y_3 - y_c) \frac{d\sigma^{(0)}}{dx_1 dx_2}, \end{aligned} \tag{3.7}$$

with y_3 given by the Born expression (3.2). The first factor in the curly brackets is the non-logarithmic coefficient $C(\alpha_s) = 1 + \mathcal{O}(\alpha_s)$, which is, in general, a function of y_3 and D, and has a finite $D \to 0$ limit. The soft factor $S(D, x_1, x_2)$ accumulates all logarithmic dependences on D, and is given by

$$S(D, x_1, x_2) = \sum_n \frac{1}{n!} \int \prod_i^n \frac{d^3 k_i}{\pi \omega_i} S_n(P_a, k_1 \dots k_n) \Theta\left(\lambda_3 - \sum_i \frac{k_{ix}^2}{\omega_i Q}\right), \tag{3.8}$$

(with $\lambda_3 = D/27\lambda_1\lambda_2$). Taking the factorised structure of S_n at two loops, this expression for $S(D, x_1, x_2)$ is accurate to SL level, see [7].

Given the factorised expression for S_n, in order to sum up the series in (3.8) in suffices to factorise the theta-function constraint by using the Mellin representation. We obtain

$$S(D, x_1, x_2) = \int \frac{d\nu}{2\pi i \nu} e^{\nu \lambda_3} \sigma(\nu, x_1, x_2), \tag{3.9}$$

where

$$\sigma(\nu, x_1, x_2) = \sum_n \frac{1}{n!} \int \prod_i^n \frac{d^3 k_i}{\pi \omega_i} e^{-\nu \frac{k_{ix}^2}{\omega_i Q}} \cdot S_n(P_a, k_1 \dots k_n) \equiv e^{-\mathcal{R}(\nu, x_1, x_2)}. \tag{3.10}$$

The contour in (3.9) runs parallel to the imaginary axis with $\mathrm{Re}\,\nu > 0$. The near-to-planar region $D \ll 1$ corresponds to the region of large Mellin variable $\nu \gg 1$.

We show that the radiator is given by a PT contribution and a NP correction

$$\mathcal{R}(\nu, x_1, x_2) = \mathcal{R}^{\mathrm{PT}}(\nu, x_1, x_2) + \delta\mathcal{R}(\nu, x_1, x_2). \tag{3.11}$$

In the next section we compute the PT contribution at SL level. In section 5 we compute $\delta\mathcal{R}$, the leading $1/Q$ correction including the effect of non-inclusiveness of the D-parameter (Milan factor).

JHEP05(2001)040

4. PT contribution at SL accuracy

To obtain the PT radiator $\mathcal{R}^{\rm PT}(\nu, x_1, x_2)$ we follow the procedure described in detail in [7] for the calculation of the T_m distribution. The present case is simpler since the hard parton recoil can be neglected. At SL level we have

$$\mathcal{R}^{\rm PT} = \frac{N_c}{2}\left(r_{13} + r_{23} - \frac{1}{N_c^2}\, r_{12}\right), \tag{4.1}$$

where

$$r_{ab}(\nu, x_1, x_2) = \int \frac{d^3k}{\pi\omega} w_{ab}(k)\,\left[1 - e^{-\nu \frac{k_x^2}{\omega Q}}\right], \qquad w_{ab}(k) = \frac{\alpha_{\rm s}(k_{t,ab}^2)}{\pi k_{t,ab}^2}, \tag{4.2}$$

with $w_{ab}(k)$ the soft distribution for the dipole ab. Here the running coupling is defined in the physical scheme [11] and $k_{t,ab}$ is the invariant transverse momentum of k with respect to the hard parton pair P_a, P_b, defined as

$$k_{t,ab}^2 = \frac{2(P_a k)(k P_b)}{(P_a P_b)}. \tag{4.3}$$

The unity in the square bracket in (4.2) takes into account the virtual corrections. The contribution from the source $u(k) = e^{-\nu k_x^2/\omega Q}$ results from the exponentiation of real emissions, see (3.10). To reach SL accuracy one needs to take into account also the correction coming from hard collinear parton splittings, which will be embodied into a redefinition of the hard scales, see later.

4.1 Explicit calculation of the PT radiator

In the laboratory frame the hard parton momenta P_a and P_b are not back-to-back and the expression of soft dipole distribution $w_{ab}(k)$ is rather cumbersome (see (4.3)). It is then natural to evaluate r_{ab} starting from its expression in the centre-of-mass frame of the dipole $P_a + P_b$,

$$\begin{aligned} P_a^* &= \frac{Q_{ab}}{2}(1,0,0,1)\,, \qquad P_b^* = \frac{Q_{ab}}{2}(1,0,0,-1)\,, \\ Q_{ab}^2 &= 2P_aP_b = Q^2(x_a + x_b - 1)\,, \end{aligned} \tag{4.4}$$

in which the distribution $w_{ab}(k)$ and the phase space are given by

$$w_{ab}(k) = \frac{\alpha_{\rm s}(\kappa^2)}{\pi\kappa^2}, \qquad \frac{d^3k}{\pi\omega} = d\kappa^2\,\frac{d\phi}{2\pi}d\eta\,, \tag{4.5}$$

with κ^2, η and ϕ the squared transverse momentum, the rapidity and the azimuthal angle of the soft gluon, respectively. To compute the dipole radiator $r_{ab}(\nu)$ we need to express the source for our observable $u(k) = e^{-\nu k_x^2/\omega Q}$ in the frame (4.4). While the variable k_x is the same in the two frames, $k_x = \kappa \sin\phi$, the gluon energy ω

in the laboratory frame (see (A.1) in appendix A) is given, in terms of the dipole c.m.s. variables

$$\omega = \kappa \left(A_{ab} \cosh(\eta + \eta_{ab}^0) - \sqrt{A_{ab}^2 - 1} \cos\phi \right), \tag{4.6}$$

with A_{ab} and η_{ab}^0 the following functions of x_a, x_b

$$A_{ab} = \frac{Q}{Q_{ab}} \sqrt{x_a x_b} = \sqrt{\frac{x_a x_b}{x_a + x_b - 1}}, \qquad \tanh \eta_{ab}^0 = \frac{x_a - x_b}{x_a + x_b}. \tag{4.7}$$

Finally, using the frame (4.4), the r_{ab} radiator can be written in the form

$$r_{ab}(\nu, x_1, x_2) = \int_0^{Q^2} \frac{d\kappa^2}{\kappa^2} \frac{\alpha_s(\kappa^2)}{\pi} \int_{-\pi}^{\pi} \frac{d\phi}{2\pi} \int_{-\eta_M}^{\eta_M} d\eta \left(1 - e^{-\nu \frac{\kappa}{Q} \tau}\right), \qquad \eta_M = \ln \frac{Q_{ab}}{\kappa}, \tag{4.8}$$

where τ is the following function of η and ϕ

$$\tau = \frac{\sin^2 \phi}{A_{ab} \cosh(\eta + \eta_{ab}^0) - \sqrt{A_{ab}^2 - 1}\, \cos\phi}. \tag{4.9}$$

Note that, since $Q_{ab} \sim Q$, to SL accuracy, we do not care for the precise upper limit in κ as long as it is of order Q.

The calculation of r_{ab} is performed in appendix B and one finds, to SL accuracy,

$$r_{ab}(\nu, x_1, x_2) = 2 \int_{Q^2/\nu}^{Q^2} \frac{d\kappa^2}{\kappa^2} \frac{\alpha_s(\kappa^2)}{\pi} \ln \frac{Q_{ab}}{\kappa} + 2 \int_{Q^2/\nu^2}^{Q^2/\nu} \frac{d\kappa^2}{\kappa^2} \frac{\alpha_s(\kappa^2)}{\pi} \ln \left(\frac{e^{\gamma_E}\, \nu\, \kappa}{2 A_{ab} Q} \right). \tag{4.10}$$

Combining together the various pieces and recalling the definition of A_{ab} in (4.7) we find the full PT radiator

$$\mathcal{R}^{\rm PT}(\nu, x_1, x_2) = C_F \left[r_1(\nu, Q_1) + r_2(\nu, Q_2) \right] + C_A\, r_3(\nu, Q_3), \tag{4.11}$$

where the contribution of the hard parton #a is given by

$$\begin{aligned} r_a(\nu, Q_a) = 2 \int_{Q^2/\nu}^{Q^2} \frac{d\kappa^2}{\kappa^2} \frac{\alpha_s(\kappa^2)}{2\pi} \ln \frac{\xi_a Q_a}{\kappa} + \\ + 2 \int_{Q^2/\nu^2}^{Q^2/\nu} \frac{d\kappa^2}{\kappa^2} \frac{\alpha_s(\kappa^2)}{2\pi} \ln \left(\frac{e^{\gamma_E}\, \nu\, \kappa\, Q_a}{2 x_a Q^2} \right). \end{aligned} \tag{4.12}$$

Here the hard scales Q_a are

$$\begin{aligned} Q_1^2 &= Q_2^2 = 2(P_1 P_2) = Q^2 (1 - x_3), \\ Q_3^2 &= \frac{2(P_1 P_3)(P_3 P_2)}{(P_1 P_2)} = Q^2 \frac{(1 - x_1)(1 - x_2)}{(1 - x_3)}. \end{aligned} \tag{4.13}$$

In (4.12) we have included into the first term the rescaling factor ξ_a

$$\xi_1 = \xi_2 = e^{-3/4}\,, \qquad \xi_3 = e^{-\beta_0/4N_c}\,, \tag{4.14}$$

to take into account the hard collinear splittings of the quark and the gluon. These constants, as well as the precise expressions for the geometry dependent scales Q_a, are important in order to incorporate in the final result (4.11) for the *radiator* all terms of the order of $\alpha_s^n \ln^{n+1}\nu$ and $\alpha_s^n \ln^n \nu$.

To first order we find

$$r_a(\nu, Q_a) = \frac{\alpha_s}{2\pi}\ln^2\left(\frac{e^{\gamma_E}\,\nu\,\xi_a\,Q_a^2}{2x_a Q^2}\right) + \cdots\,. \tag{4.15}$$

This result corresponds, at DL level, to a half of the DL radiator in the T_m case [7]. The relative factor 1/2 is due to the fact that in the T_m case the contribution to the observable is linear in the angle with respect to the event plane, while it is quadratic in the D case.

The first order contribution to the PT part of the distribution (3.7) is obtained by performing the Mellin integral in (3.9). We find

$$\frac{d\Sigma^{\rm PT}(D, y_c)}{d\ln D} = \frac{\alpha_s}{2\pi}\left\{2C_T\,\ln\frac{1}{D} + \bar{G}_{11}(y_c)\right\} + \mathcal{O}\left(\alpha_s^2\right), \tag{4.16}$$

with $C_T = 2C_F + C_A$ the sum of the colour factors — the total colour charge of the hard $q\bar{q}, g$ system. Here $\bar{G}_{11}$ is given by

$$\bar{G}_{11}(y_c) = \int dx_1 dx_2 \Theta(y_3 - y_c)\frac{d\sigma^{(0)}}{\sigma(y_c)dx_1 dx_2}\,G_{11}(x_1, x_2)\,, \tag{4.17}$$

with

$$G_{11}(x_1, x_2) = 2C_T\,\ln 27\lambda_1\lambda_2 + 2C_F\left[\ln\frac{\xi_1\,Q_1^2}{2x_1Q^2} + \ln\frac{\xi_2\,Q_2^2}{2x_2Q^2}\right] + 2C_A\,\ln\frac{\xi_3\,Q_3^2}{2x_3Q^2}\,. \tag{4.18}$$

We have checked that this function correctly describes the first non-logarithmic correction by comparing with the result of the numerical program EVENT2 [12] for $y_c = 0.025$, 0.05 and 0.1.

5. NP calculation

We follow the usual procedure [6] for computing the leading NP corrections, including two-loop order to take into account the non-inclusiveness of jet observables. We start from the PT expression (4.8) and then:

- we represent the coupling by the dispersive integral [5]

$$\frac{\alpha_s(\kappa^2)}{\kappa^2} = \int_0^\infty \frac{dm^2\,\alpha_{\rm eff}(m^2)}{(\kappa^2 + m^2)^2}\,; \tag{5.1}$$

- we substitute $\sqrt{\kappa^2+m^2}$ for the momentum κ in the source in (4.8);
- we take the leading part of the integrand for small κ and m by linearising the source
$$\left[1-e^{-\nu\frac{\sqrt{\kappa^2+m^2}}{Q}\tau}\right] \longrightarrow \nu\frac{\sqrt{\kappa^2+m^2}}{Q}\tau\,, \tag{5.2}$$
since the NP part of the "effective coupling" $\delta\alpha_{\text{eff}}(m)$ has a support only at small m;
- we multiply this expression by the Milan factor $\mathcal{M}$, computed at two-loop order, to take into account effects of non-inclusiveness of jet observables.

For the $\{ab\}$-dipole contribution this procedure gives

$$\begin{aligned}\delta r_{ab}(\nu,x_1,x_2) = \nu\mathcal{M}\int dm^2\frac{\delta\alpha_{\text{eff}}(m)}{\pi}\frac{-d}{dm^2}\int\frac{d^2\kappa}{\pi(\kappa^2+m^2)}\frac{\sqrt{\kappa^2+m^2}}{Q}\times\\ \times\int_{-\infty}^{\infty}d\eta\,\tau(\eta)\,,\end{aligned} \tag{5.3}$$

where τ is the function of x_1, x_2 defined in (4.9). It is related with the ratio of transverse momentum to energy and therefore decreases exponentially in rapidity. This allows us to extend to infinity the η integrals by setting $\eta_M=\infty$.

Here lies the main difference with the T_m case in which the observable was uniform in rapidity so that the corresponding NP radiator involved a divergent rapidity integral. There one had to keep the hard parton recoil momentum which provided an effective cutoff to the rapidity integral and resulted in a log-enhanced NP contribution.

We find the leading NP correction to the $\{ab\}$-radiator

$$\delta r_{ab}(\nu,x_1,x_2) = \nu\,\frac{a^{\text{NP}}}{Q}g_{ab}(x_1,x_2)\,, \tag{5.4}$$

where g_{ab} is the geometry dependent function

$$g_{ab}(x_1,x_2) \equiv \int_{-\pi}^{\pi}\frac{d\phi}{2\pi}\int_{-\infty}^{\infty}\frac{d\eta\sin^2\phi}{A_{ab}\cosh\eta-\cos\phi\sqrt{A_{ab}^2-1}}\,, \tag{5.5}$$

and a^{NP} is the NP parameter

$$a^{\text{NP}} = 2\mathcal{M}\int dm\frac{\delta\alpha_{\text{eff}}(m)}{\pi}\,. \tag{5.6}$$

Combining all pieces we obtain the $1/Q$ correction to the radiator

$$\delta\mathcal{R}(\nu) = \nu\,\frac{a^{\text{NP}}}{Q}\Delta(x_1,x_2)\,,\qquad \Delta = \frac{N_c}{2}\left(g_{13}+g_{23}-\frac{1}{N_c^2}\,g_{12}\right). \tag{5.7}$$

After merging the PT and NP corrections we can write the NP parameter in the form

$$a^{\rm NP} = \frac{4\mu_I}{\pi^2}\mathcal{M}\left\{\alpha_0(\mu_I) - \bar{\alpha}_s - \beta_0\,\frac{\bar{\alpha}_s^2}{2\pi}\left(\ln\frac{Q}{\mu_I}+\frac{K}{\beta_0}+1\right)\right\}, \qquad \bar{\alpha}_s = \alpha_{\overline{\rm MS}}(Q)\,, \tag{5.8}$$

where

$$\alpha_0(\mu_I) \equiv \frac{1}{\mu_I}\int_0^{\mu_I} dk\,\alpha_{\rm s}(k^2)\,.$$

The term proportional to K accounts for the mismatch between the $\overline{\rm MS}$ and the physical scheme [11] and reads

$$K = N_c\left(\frac{67}{18}-\frac{\pi^2}{6}\right)-\frac{5n_f}{9}\,. \tag{5.9}$$

For the analytical expression of the Milan factor $\mathcal{M}$ see [13]. To quantify the parameter $a^{\rm NP}$ we recall the expression for the NP shift Δ_T in the thrust distribution [6],

$$\Delta_T = 2C_F\frac{a^{\rm NP}}{Q}\,. \tag{5.10}$$

6. Final result

We are now in a position to obtain the full distribution $\Sigma(D,y_c)$ in (3.7) to the standard accuracy. First we obtain the PT expression for the soft factor $S^{\rm PT}(D,x_1,x_2)$ by performing the Mellin integral (3.9) with the PT radiator (4.11). Then, using the exact result of the $\mathcal{O}\left(\alpha_{\rm s}^2\right)$ matrix element calculation, we compute the first correction of the coefficient function $C(\alpha_{\rm s})$ in (3.7). This allows us to perform the matching of the resummed and the exact result to this order. Finally, we include the leading NP correction from (5.7).

6.1 PT resummed distribution

The PT contribution is given by

$$\begin{aligned} S^{\rm PT}(D,x_1,x_2) &= \int\frac{d\nu\,e^{\nu\lambda_3}}{2\pi i\nu}e^{-\mathcal{R}^{\rm PT}(\nu,x_1,x_2)} \simeq \frac{e^{-\mathcal{R}^{\rm PT}\left(\lambda_3^{-1},x_1,x_2\right)}}{\Gamma(1+\mathcal{R}')}\,,\\ \mathcal{R}' &\equiv -D\partial_D\,\mathcal{R}^{\rm PT}\left(D^{-1},x_1,x_2\right), \end{aligned} \tag{6.1}$$

This evaluation of the Mellin integral is accurate to SL level (see e.g. [7]). In the calculation of the logarithmic derivative of $\mathcal{R}$ the precise expression for the hard scale Q_a in $r_a(\nu,Q_a)$ is beyond SL accuracy as long as it is of order Q. We can use then Q as a common hard scale in the SL functions r', and substitute the logarithmic derivative of the radiator $\mathcal{R}'$ with

$$\mathcal{R}'_T \equiv C_T\int_{(DQ)^2}^{DQ^2}\frac{d\kappa^2}{\kappa^2}\frac{\alpha_{\rm s}(\kappa^2)}{\pi}\,, \tag{6.2}$$

where we have explicitly used the expression (4.10).

Again, to SL accuracy, we can expand the radiator in the exponent of (6.1) and write

$$\mathcal{R}^{\mathrm{PT}}\left(\lambda_3^{-1}, x_1, x_2\right) = \mathcal{R}^{\mathrm{PT}}\left(D^{-1}, x_1, x_2\right) + \mathcal{R}'_T \cdot \ln(27\lambda_1\lambda_2)\,, \tag{6.3}$$

where $\mathcal{O}(\alpha_{\mathrm{s}})$ corrections have been neglected. We conclude by giving the SL-accurate expression

$$S^{\mathrm{PT}}(D, x_1, x_2) = e^{-\mathcal{R}^{\mathrm{PT}}\left(D^{-1}, x_1, x_2\right)} \cdot \frac{e^{-\mathcal{R}'_T \ln(27\lambda_1\lambda_2)}}{\Gamma(1+\mathcal{R}'_T)}\,. \tag{6.4}$$

Using the expression of the PT radiator given in appendix B and $\mathcal{R}'_T$ given in (6.2), this distribution can be written as

$$\begin{aligned} \ln S^{\mathrm{PT}}(D, x_1, x_2) &= L\, g_1(\bar{\alpha}_s\, L) + g_2(\bar{\alpha}_s\, L, x_1, x_2)\,, \\ \bar{\alpha}_s &= \alpha_{\overline{\mathrm{MS}}}(Q)\,, \qquad L = -\ln D\,, \end{aligned} \tag{6.5}$$

where only the logarithmic terms in D were kept, while the finite corrections $\mathcal{O}(\alpha_{\mathrm{s}})$ dropped. This precaution is necessary in order to properly set up the procedure for matching the resummed expression with the exact fixed order result. The DL contribution, the first term in (6.5), does not depend on x_1, x_2. Therefore the dependence on the event geometry emerges at the level of subleading SL effects. In the first order we recover from (6.5) the result already obtained in (4.16).

Finally, the resummed PT distribution is given by

$$\Sigma^{\mathrm{PT}}(D, y_c) = \int dx_1 dx_2 \Theta(y_3 - y_c) \frac{d\sigma^{(0)}}{\sigma(y_c) dx_1 dx_2} S^{\mathrm{PT}}(D, x_1, x_2)\,. \tag{6.6}$$

6.2 Matching resummed and fixed-order predictions

Here we consider the matching with the exact result of order α_{s}^2, which allows us to compute the first order contribution to the coefficient function $C(\alpha_{\mathrm{s}})$ in (3.7). The exact first order result reads

$$\Sigma^{\mathrm{PT}}_{\mathrm{exact}}(D, y_c) = 1 + \frac{\alpha_{\mathrm{s}}}{2\pi}\left(-C_T \ln^2\frac{1}{D} - \bar{G}_{11}(y_c)\ln\frac{1}{D} + c_1(D, y_c)\right) + \mathcal{O}\left(\alpha_{\mathrm{s}}^2\right)\,, \tag{6.7}$$

where $\bar{G}_{11}(y_c)$ is defined in (4.17) and $c_1(D, y_c)$ is a function (regular at $D = 0$) which we calculate numerically by using the four-parton numerical program EVENT2 [12]. This gives

$$C(\alpha_{\mathrm{s}}) = 1 + \frac{\alpha_{\mathrm{s}}}{2\pi} c_1(D, y_c) + \cdots\,. \tag{6.8}$$

In figure 1 we report $c_1(D, y_c)$ as a function of D for three values of y_c.

We define the three matched expressions:

- Log-R matching:

$$\Sigma^{\mathrm{PT}}_{\mathrm{mat}}(D, y_c) \equiv e^{\frac{\alpha_{\mathrm{s}}}{2\pi} c_1(D, y_c)} \cdot \Sigma^{\mathrm{PT}}(D, y_c)\,, \tag{6.9}$$

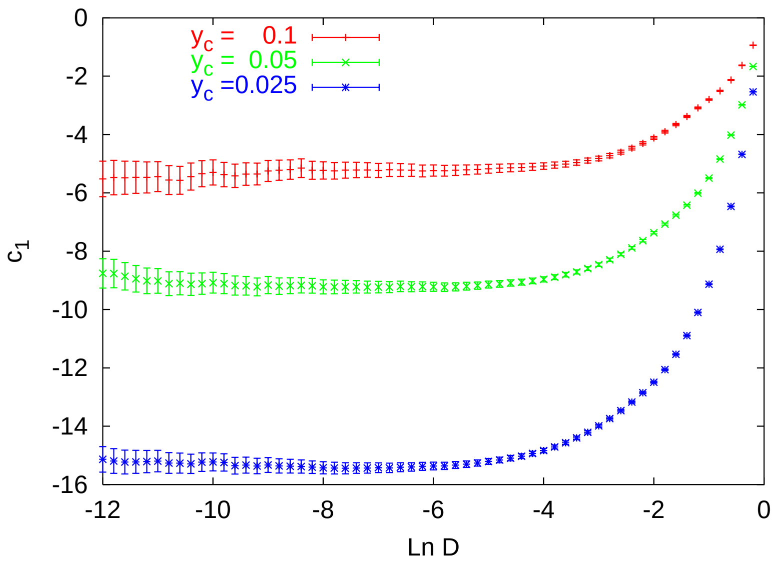

Figure 1: The first order coefficient function for three different values of y_c.

- R-matching:

$$\Sigma_{\mathrm{mat}}^{\mathrm{PT}}(D, y_c) \equiv \left(1 + \frac{\alpha_{\mathrm{s}}}{2\pi} c_1(0, y_c)\right) \cdot \Sigma^{\mathrm{PT}}(D, y_c) + \\ + \frac{\alpha_{\mathrm{s}}}{2\pi} \left(c_1(D, y_c) - c_1(0, y_c)\right), \tag{6.10}$$

- modified R-matching:

$$\Sigma_{\mathrm{mat}}^{\mathrm{PT}}(D, y_c) \equiv \left(1 + \frac{\alpha_{\mathrm{s}}}{2\pi} c_1(D, y_c)\right) \cdot \Sigma^{\mathrm{PT}}(D, y_c). \tag{6.11}$$

It is easy to see that each of these expressions reproduces the first order result (6.7) and accounts for all terms of order $\alpha_{\mathrm{s}}^n \ln^m D$ with $m \geq 2n - 2$. To obtain also the $\alpha_{\mathrm{s}}^n \ln^{2n-3} D$ terms one needs a second order matching ($\mathcal{O}(\alpha_{\mathrm{s}}^3)$ exact matrix element calculation) which requires five-parton generators [14, 15]. The matching procedure becomes more involved and will be discussed in [16].

6.3 Including NP corrections

We now consider the distribution with the NP corrections included. Using the expression (5.7) for the NP radiator, we have

$$S(D, x_1, x_2) = \int \frac{d\nu\, e^{\nu\lambda_3}}{2\pi i\nu} e^{-\left\{\nu \frac{a^{\mathrm{NP}}}{Q} \Delta + \mathcal{R}^{\mathrm{PT}}(\nu)\right\}} = S^{\mathrm{PT}}\left(D - \delta D, x_1, x_2\right), \tag{6.12}$$

where

$$\delta D = \frac{a^{\mathrm{NP}}}{Q} \cdot \mathcal{D}(x_1, x_2), \qquad \mathcal{D}(x_1, x_2) = 27\lambda_1\lambda_2\, \Delta(x_1, x_2). \tag{6.13}$$

As for other shape observables, we have embodied the leading NP correction as a $1/Q$ shift of the argument of the PT distribution. The magnitude of the shift is determined by the product of the universal NP parameter and the geometry dependent function $\mathcal{D}(x_1, x_2)$ with $\Delta(x_1, x_2)$ given in (5.7).

The final expression that includes the NP correction is given (for instance, in the Log-R matching scheme) by

$$\Sigma(D, y_c) = \int dx_1 dx_2 \Theta(y_3 - y_c) \frac{d\sigma^{(0)}}{\sigma(y_c) dx_1 dx_2} e^{\frac{\alpha_s}{2\pi} c_1(D', y_c)} \cdot S^{\rm PT}(D', x_1, x_2) , \qquad (6.14)$$

where D' is the shifted variable

$$\frac{1}{D'} = \frac{1}{D - \delta D} - \frac{1}{1 - \delta D} + 1 . \qquad (6.15)$$

The two last terms in (6.15) are relevant only at large D and have been added as to ensure the correct normalisation of the distribution, $D' = 1$ at $D = 1$.

6.4 Mean value

We can also consider the mean value of D at fixed y_c defined as

$$\langle D \rangle = \int_0^1 dD D \frac{d\Sigma(D, y_c)}{dD} . \qquad (6.16)$$

The integral is dominated by the region of finite D where the secondary partons are all hard, and out of the event plane, so that no logarithmic enhancements are involved here. The PT contribution $\langle D \rangle^{\rm PT}$ should be then obtained from a fixed order calculation. We have to add to it, however, a NP correction

$$\langle D \rangle = \langle D \rangle^{\rm PT} + \langle D \rangle^{\rm NP} . \qquad (6.17)$$

The NP correction is determined by soft (small transverse momentum) partons and can be obtained from the present analysis, cf. [7]. It is simply related with the average value of the shift as follows

$$\langle D \rangle^{\rm NP} = \frac{a^{\rm NP}}{Q} \int dx_1 dx_2 \Theta(y_3 - y_c) \frac{d\sigma^{(0)}}{\sigma(y_c) dx_1 dx_2} \cdot \mathcal{D}(x_1, x_2) , \qquad (6.18)$$

with $\mathcal{D}(x_1, x_2)$ given in (6.13).[5]

[5]The expression (6.18) has been checked by G.P. Salam and Z. Trócsanyi using their (unpublished) numerical program.

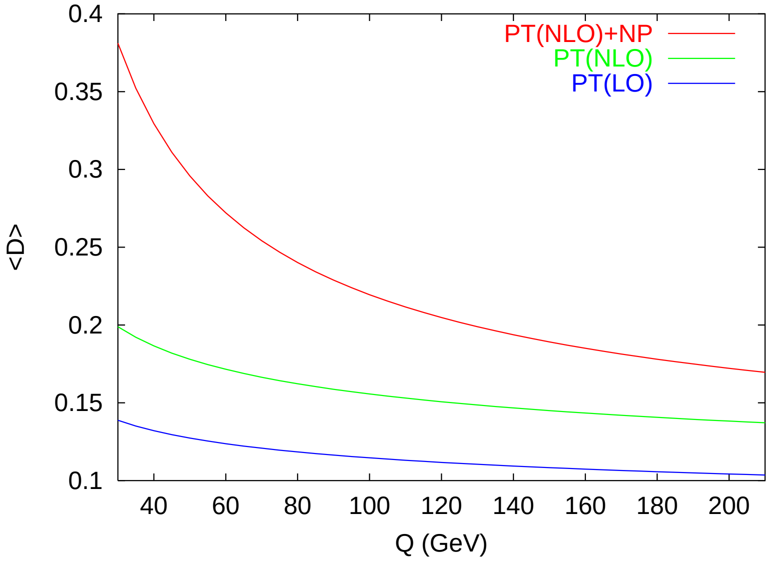

Figure 2: The mean value $\langle D \rangle$ as a function of Q for $y_c = 0.05$. Here we have taken $\alpha_{\overline{\rm MS}}(M_Z) = 0.118$ and the NP parameter $\alpha_0(2\,\text{GeV}) = 0.44$.

7. Numerical analysis

We report here the numerical results for some typical values of y_c. Data are not yet available. The results depend on the two parameters $\alpha_{\overline{\rm MS}}(M_Z)$ and $\alpha_0(\mu_I)$ (with $\mu_I = 2\,\text{GeV}$) which values we fix in the range determined by the 2-jet shape analysis, see for instance [17].

In figure 2 we plot, as a function of Q, the mean value $\langle D \rangle$ given in (6.16) for $y_c = 0.05$. The leading order PT contribution is obtained from EVENT2 [12]. The next-to-leading order PT contribution is obtained from DEBRECEN [14]. The NP contribution is given by (6.18). We see that the NP correction is large up to LEP-II energies. Actually, the coefficient $\Delta(x_1, x_2)$ of the NP correction is large due to the fact that one of the three radiating hard partons is the gluon whose contribution to the NP radiation is proportional to its large colour charge, see (5.7).

In figure 3 we plot the mean value $\langle D \rangle$ given in (6.16) for three different values of y_c at $Q = 91.2\,\text{GeV}$. The mean value decreases with y_c decreasing. This is expected since decreasing y_c one includes configurations in which the hard gluon become close to one of the quarks, so that the independent radiation off the gluon gets suppressed. In figures 4, 5 and 6 we plot the distributions $\Sigma(D, y_c)$ for three values of y_c for $Q = 91.2\,\text{GeV}$. The PT distribution is given by the first order Log-R matched expression in (6.9). (The second order matching will be presented elsewhere [16].) The full distribution is given by the expression (6.14). The PT peak is shifted to the right by an amount of order of the NP part of the mean values, see figure 3. The shift of the PT distribution is not uniform since the x_1, x_2-dependent shift has been averaged over the Born distribution.

JHEP05(2001)040

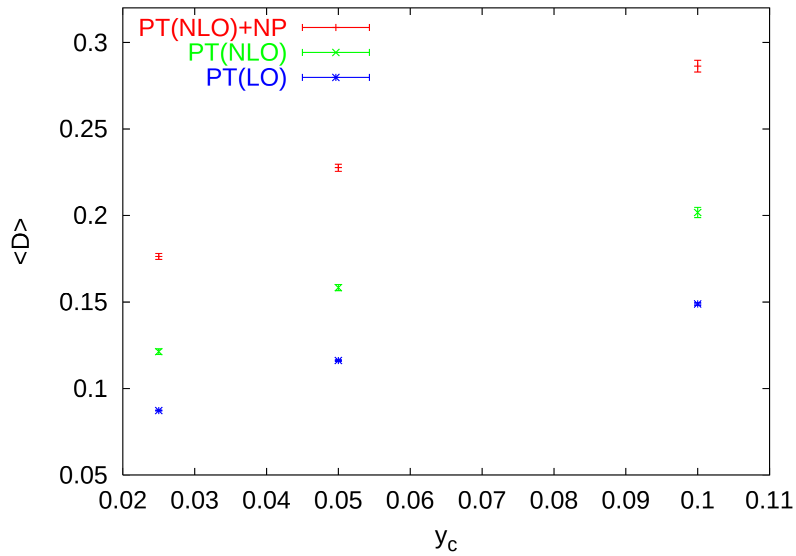

Figure 3: The mean value $\langle D \rangle$ as a function of y_c for $Q = 91.2\,\mathrm{GeV}$ for $\alpha_{\overline{\mathrm{MS}}}(M_Z)$ and $\alpha_0(\mu_I)$ taken at the values of the previous figure.

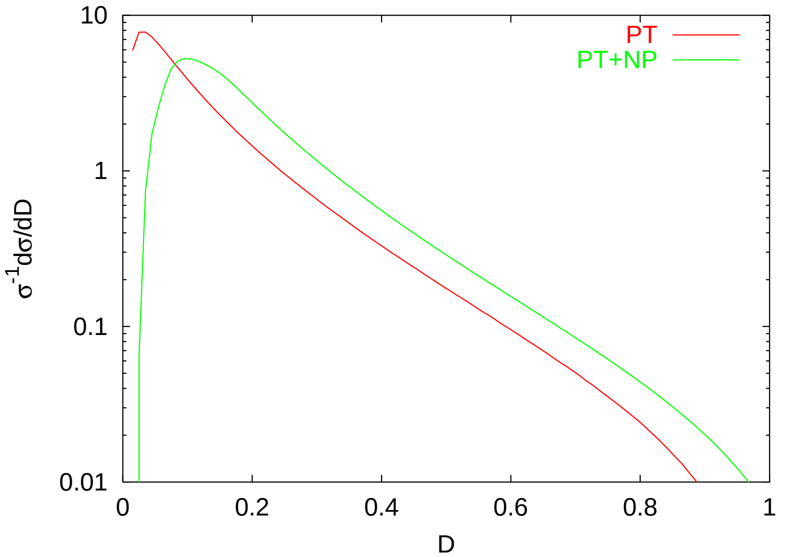

Figure 4: The distribution for $Q = 91.2\,\mathrm{GeV}$ and $y_c = 0.025$ for $\alpha_{\overline{\mathrm{MS}}}(M_Z) = 0.118$ and the NP parameter $\alpha_0(\mu_I) = 0.52$ at $\mu_I = 2\,\mathrm{GeV}$.

8. Discussion and conclusion

The aim of the present study is the understanding of the structure of multi-jet events in e^+e^-. To master this field is important, especially, for hadron-hadron collisions where the QCD events involve more than two jets.

This is the second near-to-planar three-jet shape variable, after T_m, studied at an accuracy sufficient to make quantitative predictions (SL resummation, matching with fixed order, NP corrections). The main difference between the D-parameter

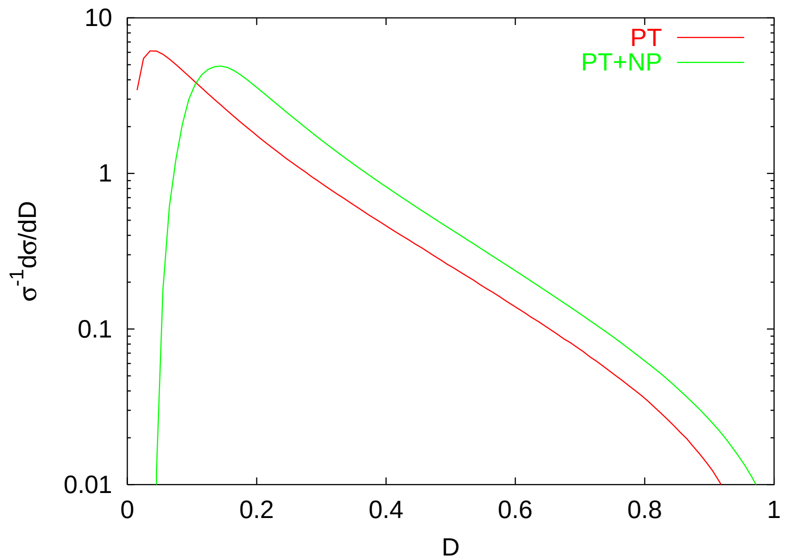

Figure 5: The distribution for $Q = 91.2\,\mathrm{GeV}$ and $y_c = 0.5$ for $\alpha_{\overline{\mathrm{MS}}}(M_Z) = 0.118$ and the NP parameter $\alpha_0(\mu_I) = 0.52$ at $\mu_I = 2\,\mathrm{GeV}$.

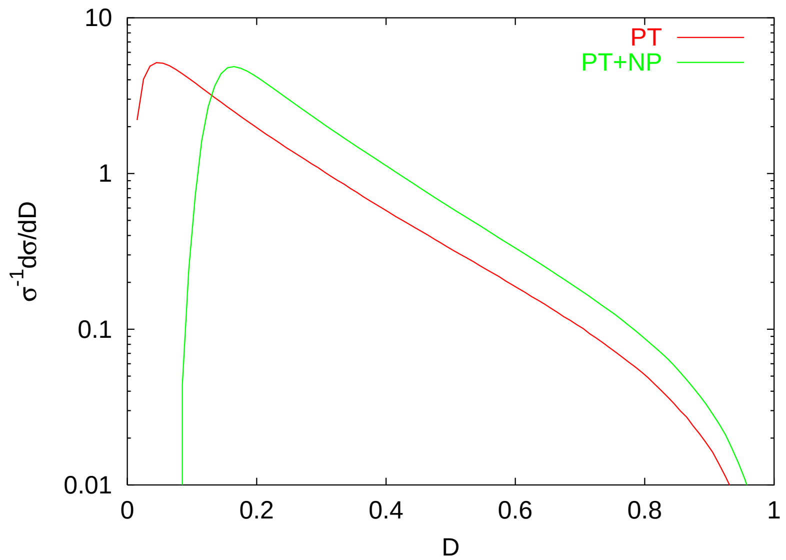

Figure 6: The distribution for $Q = 91.2\,\mathrm{GeV}$ and $y_c = 0.1$ for $\alpha_{\overline{\mathrm{MS}}}(M_Z) = 0.118$ and the NP parameter $\alpha_0(\mu_I) = 0.52$ at $\mu_I = 2\,\mathrm{GeV}$.

and T_m is the dependence of the observable on particle rapidity. Actually, T_m is uniform in rapidity, while D is exponentially dumped. This feature has important consequences both at PT and NP level.

On the PT side, the hard parton recoil explicitly enters the observable in the T_m case. On the contrary, in the D case it gives rise to corrections beyond SL accuracy. This in turn implies that the PT D distribution depends only on the geometry of the event (the angles between jets) and not on its colour configuration.

In what concerns NP corrections, one finds that in the D case only soft radiation at large angles contributes to the NP shift. As a consequence, the shift is not logarithmically enhanced, as was the case of T_m. This is the same difference that occurs between $1-T, C, M^2/Q^2$ and B jet shapes in the two-jet case.

We observe that the shift for the D parameter is larger than is typical for 2-jet observables. This is explained by the fact that in 3-jet events we have three hard radiating partons whose total colour charge $2C_F + C_A$ is significantly larger than $2C_F$, the total colour charge of a two-jet system. As a consequence, while for 2-jet observables higher order NP effects come into play below the peak of the distribution, for the D parameter they are already relevant in the proximity of the peak. This calls for a deeper analysis that would address higher powers in $1/Q$, for example, along the lines of Korchemsky-Sterman approach which was recently developed for some 2-jet observables in [18]. The comparison with experimental data (not yet available) would shed light on this important point.

Near-to-planar 3-jet events provide a new method to measure the fundamental QCD parameter $\alpha_s(M_Z)$ and to have a further test of the universality of genuine NP effects in jet physics.

Acknowledgments

We are grateful to Gavin Salam and Bryan Webber for helpful discussions and suggestions. We thank also Günther Dissertori and Oliver Passon for discussions on future analyses of LEP data.

A. Born kinematics

We select the event plane in such a way that the two Born momenta with the maximum and minimum x-component are given by

$$P_{\max} = E(x_{\max}, 0, 0, x_{\max}), \qquad P_{\min} = E(x_{\min}, 0, -T_M, -t_{\min}). \tag{A.1}$$

with $Q = 2E$ and

$$\begin{aligned} &x_{\max} = T, \qquad x_{\min} = 1 - \frac{T}{2}(1+\rho), \qquad t_{\min} = \frac{T}{2} - \rho\left(1 - \frac{T}{2}\right), \\ &\rho \equiv \sqrt{1 - \frac{T_M^2}{1-T}}, \end{aligned} \tag{A.2}$$

so that the thrust major is

$$T_M = \frac{2}{x_{\max}}\sqrt{(1-x_1)(1-x_2)(1-x_3)}. \tag{A.3}$$

To define these massless momenta one needs that T and T_M are restricted to the region

$$\frac{2(1-T)\sqrt{2T-1}}{T} < T_M < \sqrt{1-T}\,. \tag{A.4}$$

In this paper we consider T, T_M restricted to this region.

B. The PT radiator

Here we compute the radiator component $r_{ab}(\nu)$ given in (4.8). We change integration variable from η to τ with the Jacobian

$$d\eta = -\frac{d\tau}{\tau}\,K(\tau)\,, \qquad K(\tau) = \frac{\sin^2\phi}{\sqrt{\left(\sin^2\phi + \tau\sqrt{A^2-1}\,\cos\phi\right)^2 - \tau^2 A^2}}\,. \tag{B.1}$$

In this appendix we set $A_{ab} \to A$ and $\eta^0_{ab} \to \eta_0$ defined in (4.7). The η-integral can be divided into the positive and negative rapidity regions and one has

$$r_{ab}(\nu) = r^+_{ab}(\nu) + r^-_{ab}(\nu)\,, \tag{B.2}$$

where

$$r^\pm_{ab}(\nu) = 2\int_0^Q \frac{d\kappa}{\kappa}\frac{\alpha_{\mathrm{s}}(\kappa^2)}{\pi}\int_{-\pi}^{\pi}\frac{d\phi}{2\pi}\int_{\tau^\pm_M}^{\tau_0}\frac{d\tau}{\tau}\,K(\tau)\left(1-e^{-\nu\frac{\kappa}{Q}\tau}\right). \tag{B.3}$$

The limits are for $\eta = \pm\eta_0$ and $\eta = \eta_M$

$$\tau_0 = \frac{\sin^2\phi}{A-\sqrt{A^2-1}\,\cos\phi}\,, \qquad \tau^\pm_M = \frac{\sin^2\phi}{A\cosh(\eta_M \pm \eta_0) - \sqrt{A^2-1}\,\cos\phi}\,. \tag{B.4}$$

The limit $\tau^\pm_M$ is a function of κ given, for small κ, by

$$\tau^\pm_M(\kappa) \simeq \frac{2\sin^2\phi}{A}\frac{\kappa}{Q^\pm_{ab}}\,, \qquad Q^\pm_{ab} = Q_{ab}e^{\pm\eta_0}\,. \tag{B.5}$$

In (B.3) we can substitute, to SL accuracy, the factor $[1-e^{-\nu\frac{\kappa}{Q}\tau}]$ by the effective cutoff (C.4) and we obtain

$$r^\pm_{ab}(\nu) \simeq 2\int_0^Q \frac{d\kappa}{\kappa}\frac{\alpha_{\mathrm{s}}(\kappa^2)}{\pi}\int_{-\pi}^{\pi}\frac{d\phi}{2\pi}\int_{\tau^\pm_M}^{\tau_0}\frac{d\tau}{\tau}\,K(\tau)\vartheta\left(\tau-\frac{Q}{\bar{\nu}\kappa}\right). \tag{B.6}$$

In order to reach SL accuracy, we have to take the running coupling at two loops and include the non-soft part of the parton splitting function. Before discussing this case, it is instructive to consider the first order term in $\alpha_{\mathrm{s}} = \alpha_{\mathrm{s}}(Q)$.

B.1 First order result

We change again variables $q = \kappa\tau$ and obtain

$$r_{ab}^{\pm} = \frac{2\alpha_s}{\pi}\int_{Q/\bar{\nu}}^{Q}\frac{dq}{q}\int_{-\pi}^{\pi}\frac{d\phi}{2\pi}\int_{\tau_\pm}^{\tau_0}\frac{d\tau}{\tau}K(\tau)\,, \tag{B.7}$$

where $\tau_\pm$ is the solution of the equation

$$\tau_\pm = \tau_M^{\pm}\left(\frac{q}{\tau_\pm}\right) = \sqrt{\frac{2\sin^2\phi}{A}\frac{q}{Q_{ab}^{\pm}}} + \mathcal{O}\left(\frac{q}{Q}\right), \tag{B.8}$$

with $\tau_M^{\pm}(k)$ the function of κ given in (B.4). Again in (B.7) we take as upper limit the hard scale Q. For small q the τ integral is

$$\int_{\tau_\pm}^{\tau_0}\frac{d\tau}{\tau}K(\tau) = \frac{1}{2}\ln\frac{2\,Q_{ab}^{\pm}}{Aq} + \frac{1}{2}\ln\sin^2\phi + \mathcal{O}\left(\frac{q}{Q}\right).$$

Summing the r_{ab}^{+} and r_{ab}^{-} contributions, we get, at SL accuracy,

$$r_{ab}(\nu) \simeq \frac{2\alpha_s}{\pi}\int_{Q/\bar{\nu}}^{Q}\frac{dq}{q}\ln\frac{Q_{ab}}{2Aq} \simeq \frac{\alpha_s}{\pi}\ln^2\left(\frac{\bar{\nu}Q_{ab}^2}{2\sqrt{x_a x_b}Q^2}\right). \tag{B.9}$$

Finally, using (4.1) we obtain, for fixed α_s, the complete radiator $\mathcal{R}^{\rm PT}(\nu)$ in (4.11). The parton $\#a$ component in (4.15) is obtained from (B.9) by taking into account the non-soft part of the splitting function which gives the rescaling factors ξ_a in (4.14).

B.2 SL result

Here we evaluate $r_{ab}^{\pm}$ in (B.6) with the running coupling at two loops. We consider the two regions of the τ-integration: $\tau_M^{\pm} > Q/\bar{\nu}\kappa$ and $\tau_M^{\pm} < Q/\bar{\nu}\kappa$. We then have two contributions

$$\begin{aligned}
r_{ab}^{\pm} &= 2\int_{-\pi}^{\pi}\frac{d\phi}{2\pi}\left\{\int_{q_\pm}^{Q}\frac{d\kappa}{\kappa}\frac{\alpha_s(\kappa^2)}{\pi}\int_{\tau_M^{\pm}}^{\tau_0}\frac{d\tau}{\tau}K(\tau) + \int_{\frac{Q}{\bar{\nu}\tau_0}}^{q_\pm}\frac{d\kappa}{\kappa}\frac{\alpha_s(\kappa^2)}{\pi}\int_{\frac{Q}{\bar{\nu}\kappa}}^{\tau_0}\frac{d\tau}{\tau}K(\tau)\right\} \qquad (\text{B.10})\\
&\simeq 2\int_{-\pi}^{\pi}\frac{d\phi}{2\pi}\left\{\int_{q_\pm}^{Q}\frac{d\kappa}{\kappa}\frac{1}{\pi}\left(\alpha_s(\kappa^2) + \alpha_s\left(\frac{q_\pm^4}{\kappa^2}\right)\right)\ln\frac{Q_{ab}^{\pm}}{\kappa}\right\}, \qquad q_\pm^2 = \frac{QQ_{ab}^{\pm}A_{ab}}{\bar{\nu}\,2\sin^2\phi}\,,
\end{aligned}$$

where in the second term we made the variable change $\kappa \to q_\pm^2/\kappa$. The precise expression of the upper limit in the first term is beyond SL accuracy as long as of order Q. In the second line we have neglected terms beyond SL accuracy ($\alpha_s^n \ln^{n-1}\nu$).

Now we can perform the ϕ-integration observing that only terms containing one power of $\ln\sin^2\phi$ contribute to the radiator at SL level. Therefore we make the substitution

$$\int_{-\pi}^{\pi}\frac{d\phi}{2\pi}\ln\sin^2\phi = -\ln 4 \Longrightarrow q_\pm^2 \longrightarrow q_\pm^2 = \frac{QQ_{ab}^{\pm}\,2A_{ab}}{\bar{\nu}}\,,$$

In conclusion the radiator may be written as

$$r_{ab}^{\pm} = 2\int_{q_{\pm}^2}^{Q^2} \frac{d\kappa^2}{\kappa^2}\frac{\alpha_{\mathrm{s}}(\kappa^2)}{2\pi}\ln\frac{Q_{ab}^{\pm}}{\kappa} + 2\int_{q_{\pm}^4/Q^2}^{q_{\pm}^2} \frac{d\kappa^2}{\kappa^2}\frac{\alpha_{\mathrm{s}}(\kappa^2)}{2\pi}\ln\frac{\bar{\nu}\,\kappa}{2A_{ab}Q}\,. \tag{B.11}$$

One finds that the dependence on $q_{\pm}$ in the integration limits cancels out, so that, adding r_{ab}^{+} and r_{ab}^{-}, one is left with (4.10). Combining together the various pieces and recalling the definition of A_{ab} in (4.7) we find the full radiator $\mathcal{R}^{\mathrm{PT}}(\nu)$ in (4.11) with the parton $\#a$ component r_a given by the sum of two terms

$$\begin{aligned} r_a &= r_a^U + r_a^L\,, \\ r_a^U &= 2\int_{Q^2/\nu}^{Q^2} \frac{d\kappa^2}{\kappa^2}\frac{\alpha_{\mathrm{s}}(\kappa^2)}{2\pi}\ln\frac{\xi_a Q_a}{\kappa}\,, \\ r_a^L &= 2\int_{Q^2/\nu^2}^{Q^2/\nu} \frac{d\kappa^2}{\kappa^2}\frac{\alpha_{\mathrm{s}}(\kappa^2)}{2\pi}\ln\left(\frac{\bar{\nu}\,\kappa\,Q_a}{2x_a Q^2}\right). \end{aligned} \tag{B.12}$$

The hard scales are given by (4.13). The SL terms coming from the parton hard collinear splitting are taken into account, see [7, 19], simply by rescaling the scale Q_a by the constants ξ_a in (4.14) in the piece r_a^U. To first order in α_{s} this expression coincides with the result in (4.15).

To evaluate the two components r_a^U, r_a^L it is enough to consider the following expression for the running coupling:

$$\alpha_{\mathrm{s}}(\mu^2) = \frac{\alpha_{\mathrm{s}}}{1-\lambda}\left(1 - \frac{\beta_1}{\beta_0}\frac{\alpha_{\mathrm{s}}}{2\pi}\frac{\ln(1-\lambda)}{1-\lambda}\right), \qquad \lambda = \frac{\alpha_{\mathrm{s}}\beta_0}{4\pi}\ln\frac{Q^2}{\mu^2}\,, \tag{B.13}$$

with

$$\beta_0 = \frac{11N_c - 2n_f}{3}\,, \qquad \beta_1 = \frac{17N_c^2 - 5N_c\,n_f - 3C_F\,n_f}{3}\,, \tag{B.14}$$

and $\alpha_{\mathrm{s}} = \alpha_{\mathrm{s}}(Q)$ in the physical scheme [11] related to the $\overline{\mathrm{MS}}$ by

$$\alpha_{\mathrm{s}} = \bar{\alpha}_{\mathrm{s}}\left(1 + \frac{K\bar{\alpha}_{\mathrm{s}}}{2\pi} + \cdots\right), \qquad \bar{\alpha}_{\mathrm{s}} = \alpha_{\overline{\mathrm{MS}}}(Q)\,, \tag{B.15}$$

with K given in (5.9).

We can separate the pieces depending on the geometry. We write

$$r_a^U = r_{\mathrm{DL}}^U + r_{\mathrm{SL}}^U \cdot \ln\left(\frac{\xi_a Q_a}{Q}\right)^2, \qquad r_a^L = r_{\mathrm{DL}}^L + r_{\mathrm{SL}}^L \cdot \ln\left(\frac{e^{\gamma_E} Q_a}{2x_a Q}\right)^2. \tag{B.16}$$

Here the geometry dependence is explicitly expressed by the scales Q_a, while the various r-functions are evaluated at the common hard scale Q. The various functions are

$$r_{\rm DL}^U = \int_{Q^2/\nu}^{Q^2} \frac{d\kappa^2}{\kappa^2}\frac{\alpha_{\rm s}(\kappa^2)}{2\pi}\ln\frac{Q^2}{\kappa^2} = \frac{8\pi}{\bar\alpha_{\rm s}\beta_0^2}\left(-\rho - L(\rho)\right) - \frac{4\beta_1}{\beta_0^3}\left(\frac{1}{2}L^2(\rho)+\frac{L(\rho)+\rho}{1-\rho}\right)+$$
$$+\frac{4K}{\beta_0^2}\left(L(\rho)+\frac{\rho}{1-\rho}\right),$$
$$r_{\rm DL}^L = \int_{Q^2/\nu^2}^{Q^2/\nu} \frac{d\kappa^2}{\kappa^2}\frac{\alpha_{\rm s}(\kappa^2)}{2\pi}\ln\frac{\nu^2\kappa^2}{Q^2} = \frac{8\pi}{\bar\alpha_{\rm s}\beta_0^2}\left(\rho + (2\rho-1)(L(\rho)-L(2\rho))\right) -$$
$$-\frac{4\beta_1}{\beta_0^3}\left(\frac{1}{2}\left(L^2(\rho)-L^2(2\rho)\right)+(2\rho-1)\left(\frac{L(2\rho)+2\rho}{1-2\rho}-\frac{L(\rho)+\rho}{1-\rho}\right)\right)+$$
$$+\frac{4K}{\beta_0^2}\left(L(\rho)-L(2\rho)-\frac{\rho}{1-\rho}\right),$$
$$r_{\rm SL}^U = \int_{Q^2/\nu}^{Q^2} \frac{d\kappa^2}{\kappa^2}\frac{\alpha_{\rm s}(\kappa^2)}{2\pi} = \frac{2}{\beta_0}\ln\frac{1}{1-\rho},$$
$$r_{\rm SL}^L = \int_{Q^2/\nu^2}^{Q^2/\nu} \frac{d\kappa^2}{\kappa^2}\frac{\alpha_{\rm s}(\kappa^2)}{2\pi} = \frac{2}{\beta_0}\ln\frac{1-\rho}{1-2\rho}, \tag{B.17}$$

where

$$\rho = \bar\alpha_{\rm s}\frac{\beta_0}{4\pi}\ln\nu\,, \qquad L(x)=\ln(1-x)\,. \tag{B.18}$$

Notice that the radiator contain only DL and SL terms

$$\mathcal{R}^{\rm PT}(\nu) = \frac{1}{\alpha_{\rm s}}F_1(\rho)+F_2(\rho)\,. \tag{B.19}$$

C. Effective cutoff

Performing the variable change $q=\kappa\tau$ in (B.3) the radiator is proportional to

$$r(Q) = \int_0^Q \frac{dq}{q}\left(1-e^{-\nu\frac{q}{Q}}\right)I(q)\,, \qquad I(q) = \int_{-\pi}^{\pi}\frac{d\phi}{2\pi}\int_{\tau_\pm}^{\tau_0}\frac{d\tau}{\tau}K(\tau)\alpha_{\rm s}\left(\frac{q^2}{\tau^2}\right). \tag{C.1}$$

This shows that $I(q)$ has the form

$$I(q) = F(\alpha_{\rm s}L_q)+\alpha_{\rm s}G(\alpha_{\rm s}L_q)+\cdots\,, \qquad \alpha_{\rm s}=\alpha_{\rm s}(Q)\,, \qquad L_q = \ln\frac{Q}{q}\,, \tag{C.2}$$

where the dots do not contribute at SL level. We consider first the contribution from the leading piece of $I(q)$

$$r'(Q) = \int_0^Q \frac{dq}{q}\left(1-e^{-\nu\frac{q}{Q}}\right)F(\alpha_{\rm s}L_q)\,. \tag{C.3}$$

To SL accuracy here we can make the substitution

$$\left(1-e^{-\nu\frac{q}{Q}}\right)\longrightarrow \vartheta\left(q-\frac{Q}{\bar\nu}\right), \qquad \bar\nu = e^{\gamma_E}\nu\,. \tag{C.4}$$

For completeness we prove this well known result (see [3]). We can write

$$r'(Q) = \int_{\bar q}^{Q} \frac{dq}{q}\, F(\alpha_s L_q) + \Delta(\bar q)\,, \tag{C.5}$$

with

$$\begin{aligned}\Delta(\bar q) &= \int_0^{\bar q} \frac{dq}{q} \left(\frac{q}{Q}\right)^{\epsilon} F(\alpha_s L_q) - \int_0^{Q} \frac{dq\, e^{-\nu\frac{q}{Q}}}{q} \left(\frac{q}{Q}\right)^{\epsilon} F(\alpha_s L_q) \\ &= F(-\alpha_s \partial_\epsilon) \cdot \left\{ \int_0^{\bar q} \frac{dq}{q} \left(\frac{q}{Q}\right)^{\epsilon} - \int_0^{Q} \frac{dq\, e^{-\nu\frac{q}{Q}}}{q} \left(\frac{q}{Q}\right)^{\epsilon} \right\}.\end{aligned} \tag{C.6}$$

for $\epsilon \to 0$. We can extend the last integral to infinity and get, up to $e^{-\nu}$ corrections for large ν,

$$\Delta(\bar q) \simeq F(-\alpha_s \partial_\epsilon) \cdot \left\{ \frac{1}{\epsilon} \left(\frac{\bar q}{Q}\right)^{\epsilon} - \frac{\Gamma(1+\epsilon)}{\epsilon} \nu^{-\epsilon} \right\}. \tag{C.7}$$

Our aim now is to select $\bar q$ in such a way that Δ is beyond SL accuracy. Setting $\bar q = Q/\bar\nu$ we get

$$\Delta(\bar q) = F(\alpha_s L_{\bar q} - \alpha_s \partial_\epsilon) \cdot f(\epsilon)\,, \qquad L_{\bar q} = -\ln \bar\nu\,. \tag{C.8}$$

where

$$f(\epsilon) = \frac{1 - \Gamma(1+\epsilon)\, e^{\epsilon \gamma_E}}{\epsilon} = \mathcal{O}(\epsilon)\,. \tag{C.9}$$

We conclude then that

$$\Delta(\bar q) \sim \alpha_s\, F'(\alpha_s L_{\bar q})\,, \qquad F'(x) = \partial_x F(x)\,, \tag{C.10}$$

which is negligible within SL accuracy. We conclude then, to SL accuracy,

$$r'(Q) \simeq \int_{Q/\bar\nu}^{Q} \frac{dq}{q}\, F(\alpha_s L_q)\,. \tag{C.11}$$

For the second term $\alpha_s G(\alpha_s L_q)$ in (C.2) the analysis is simpler. Since it gives only a SL contribution the lower scale can be taken at any value of the order Q/ν. We then conclude that to compute the radiator to SL accuracy we can use the cutoff substitution (C.4).

References

[1] P.A.M. Fernandez, O. Biebel and S. Bethke, *Tests of power corrections to event shape distributions from e^+e^- annihilation*, paper contributed to the EPS-HEP99 conference in Tampere, Finland, hep-ex/9906033;
H. Stenzel, *Power corrections to e^+ e^- event shape variables*, MPI-PHE-99-09 Prepared for 34th Rencontres de Moriond *QCD and hadronic interactions*, Les Arcs,

France, 20-27 Mar 1999;
ALEPH collaboration, *QCD measurements in e^+e^- annihilations at centre-of-mass energies between 189 and 202 GeV*, ALEPH 2000-044 CONF 2000-027;
DELPHI collaboration, *Energy dependence of event shapes and of α_s at LEP2*, *Phys. Lett.* **B 456** (1999) 322;
DELPHI collaboration, *The running of the strong coupling and a study of power corrections to hadronic event shapes with the DELPHI detector at LEP*, DELPHI 2000-116 CONF 415, July 2000;
L3 collaboration, *QCD studies in e^+e^- annihilation from 30 GeV to 189 GeV*, *Phys. Lett.* **B 489** (2000) 65 [hep-ex/0005045].

[2] ALEPH collaboration, *Measurement of α_s in hadronic Z decays using all orders resummed predictions*, *Phys. Lett.* **B 284** (1992) 163;
CELLO collaboration, *Model independent limits on λ (QCD) from e^+e^- annihilation in the energy range from 14 GeV to 46 GeV*, *Z. Physik* **C 44** (1989) 63;
DELPHI collaboration, *Consistent measurements of α_s from precise oriented event shape distributions*, *Eur. Phys. J.* **C 14** (2000) 557 [hep-ex/0002026];
JADE collaboration, P.A.M. Fernandez, O. Biebel, S. Bethke, S. Kluth and P. Pfeifenschneider, *A study of event shapes and determinations of α_s using data of e^+e^- annihilations at $\sqrt{s} = 22$ GeV to 44 GeV*, *Eur. Phys. J.* **C 1** (1998) 461 [hep-ex/9708034];
L3 collaboration, *Study of hadronic events and measurements of α_s between 30 GeV and 91 GeV*, *Phys. Lett.* **B 411** (1997) 339;
Mark II collaboration, *Determination of α_s from energy-energy correlations in e^+e^- annihilation at 29 GeV*, *Phys. Rev.* **D 37** (1988) 3091;
OPAL collaboration, *A determination of $\alpha_s(M_{Z^0})$ at LEP using resummed QCD calculations*, *Z. Physik* **C 59** (1993) 1; *QCD studies with e^+e^- annihilation data at 130 GeV and 136 GeV*, *Z. Physik* **C 72** (1996) 191; *QCD studies with e^+e^- annihilation data at 161 GeV*, *Z. Physik* **C 75** (1997) 193;
PLUTO collaboration, *Energy dependence of jet measures in e^+e^- annihilation*, *Z. Physik* **C 12** (1982) 297;
SLD collaboration, *Measurement of $\alpha_s(M_{Z^0})$ from hadronic event observables at the Z^0 resonance*, *Phys. Rev.* **D 51** (1995) 962 [hep-ex/9501003];
TASSO collaboration, *Analysis of multi-jet final states in e^+e^- annihilation*, *Phys. Lett.* **B 214** (1988) 286; *Experimental study of jet masses in e^+e^- annihilation at c.m. energies between 12 GeV and 43.5 GeV*, *Z. Physik* **C 45** (1989) 11; *Global jet properties at 14 GeV to 44 GeV center-of-mass energy in e^+e^- annihilation*, *Z. Physik* **C 47** (1990) 187;
TOPAZ collaboration, *Measurements of α_s in e^+e^- annihilation at $\sqrt{s} = 53.3$ GeV and 59.5 GeV*, *Phys. Lett.* **B 227** (1989) 495; *Experimental study of B-quark jets in e^+e^- annihilation at Tristan*, *Phys. Lett.* **B 278** (1992) 506; *Measurements of α_s in e^+e^- annihilation at Tristan*, *Phys. Lett.* **B 313** (1993) 475.

[3] S. Catani, L. Trentadue, G. Turnock and B.R. Webber, *Resummation of large logarithms in e^+e^- event shape distributions*, *Nucl. Phys.* **B 407** (1993) 3;

S. Catani, G. Turnock and B.R. Webber, *Jet broadening measures in e^+e^- annihilation*, *Phys. Lett.* **B 295** (1992) 269;
S. Catani and B.R. Webber, *Resummed C-parameter distribution in e^+e^- annihilation*, *Phys. Lett.* **B 427** (1998) 377 [hep-ph/9801350];
Y.L. Dokshitzer, A. Lucenti, G. Marchesini and G.P. Salam, *On the QCD analysis of jet broadening*, *J. High Energy Phys.* **01** (1998) 011 [hep-ph/9801324].

[4] B.R. Webber, *Estimation of power corrections to hadronic event shapes*, *Phys. Lett.* **B 339** (1994) 148 [hep-ph/9408222];
see also B.R. Webber, *Hadronization* in *Proceedings Summer School on hadronic aspects of collider physics*, Zuoz, Switzerland, August 1994, M.P. Locher ed., PSI, Villigen 1994 [hep-ph/9411384];
M. Beneke and V.M. Braun, *Power corrections and renormalons in Drell-Yan production*, *Nucl. Phys.* **B 454** (1995) 253 [hep-ph/9506452];
Y.L. Dokshitzer and B.R. Webber, *Calculation of power corrections to hadronic event shapes*, *Phys. Lett.* **B 352** (1995) 451 [hep-ph/9504219];
R. Akhoury and V.I. Zakharov, *On the universality of the leading $1/Q$ power corrections in QCD*, *Phys. Lett.* **B 357** (1995) 646 [hep-ph/9504248];
R. Akhoury and V.I. Zakharov, *Leading power corrections in QCD: from renormalons to phenomenology*, *Nucl. Phys.* **B 465** (1996) 295 [hep-ph/9507253];
G.P. Korchemsky and G. Sterman, *Nonperturbative corrections in resummed cross-sections*, *Nucl. Phys.* **B 437** (1995) 415 [hep-ph/9411211];
Y.L. Dokshitzer, V.A. Khoze and S.I. Troian, *Specific features of heavy quark production. LPHD approach to heavy particle spectra*, *Phys. Rev.* **D 53** (1996) 89 [hep-ph/9506425];
P. Nason and B.R. Webber, *Non-perturbative corrections to heavy quark fragmentation in e^+e^- annihilation*, *Phys. Lett.* **B 395** (1997) 355 [hep-ph/9612353];
P. Nason and M.H. Seymour, *Infrared renormalons and power suppressed effects in e^+e^- jet events*, *Nucl. Phys.* **B 454** (1995) 291 [hep-ph/9506317];
G.P. Korchemsky, G. Oderda and G. Sterman, *Power corrections and nonlocal operators*, hep-ph/9708346;
Y.L. Dokshitzer, G. Marchesini and B.R. Webber, *Non-perturbative effects in the energy-energy correlation*, *J. High Energy Phys.* **07** (1999) 012 [hep-ph/9905339];
M. Beneke, *Renormalons*, *Phys. Rep.* **317** (1999) 1 [hep-ph/9807443].

[5] Y.L. Dokshitzer, G. Marchesini and B.R. Webber, *Dispersive approach to power-behaved contributions in QCD hard processes*, *Nucl. Phys.* **B 469** (1996) 93 [hep-ph/9512336].

[6] Y.L. Dokshitzer, A. Lucenti, G. Marchesini and G.P. Salam, *Universality of $1/Q$ corrections to jet-shape observables rescued*, *Nucl. Phys.* **B 511** (1998) 396 [hep-ph/9707532];
Y.L. Dokshitzer, A. Lucenti, G. Marchesini and G.P. Salam, *On the universality of the Milan factor for $1/Q$ power corrections to Jet shapes*, *J. High Energy Phys.* **05** (1998) 003 [hep-ph/9802381];

Y.L. Dokshitzer, G. Marchesini and G.P. Salam, *Revisiting non-perturbative effects in the jet broadenings*, *Eur. Phys. J. Direct* **C3** (1999) 1 [hep-ph/9812487].

[7] A. Banfi, G. Marchesini, Y.L. Dokshitzer and G. Zanderighi, *QCD analysis of near-to-planar 3-jet events*, *J. High Energy Phys.* **07** (2000) 002 [hep-ph/0004027]; *Near-to-planar 3-jet events in and beyond QCD perturbation theory*, *Phys. Lett.* **B 508** (2001) 269 [hep-ph/0010267]; *Non-perturbative QCD analysis of near-to-planar three-jet events*, *J. High Energy Phys.* **03** (2001) 007 [hep-ph/0101205].

[8] G. Parisi, *Super inclusive cross-sections*, *Phys. Lett.* **B 74** (1978) 65;
J.F. Donoghue, F.E. Low and S.-Y. Pi, *Tensor analysis of hadronic jets in quantum chromodynamics*, *Phys. Rev.* **D 20** (1979) 2759;
R.K. Ellis, D.A. Ross and A.E. Terrano, *The perturbative calculation of jet structure in e^+e^- annihilation*, *Nucl. Phys.* **B 178** (1981) 421.

[9] S. Bethke, Z. Kunszt, D.E. Soper and W.J. Stirling, *New jet cluster algorithms: next-to-leading order QCD and hadronization corrections*, *Nucl. Phys.* **B 370** (1992) 310.

[10] S. Catani, Yu.L. Dokshitzer, M. Olsson, G. Turnock and B.R. Webber, *New clustering algorithm for multi-jet cross-sections in e^+e^- annihilation*, *Phys. Lett.* **B 269** (1991) 432.

[11] S. Catani, B.R. Webber and G. Marchesini, *QCD coherent branching and semiinclusive processes at large x*, *Nucl. Phys.* **B 349** (1991) 635.

[12] S. Catani and M.H. Seymour, *The dipole formalism for the calculation of QCD jet cross sections at next-to-leading order*, *Phys. Lett.* **B 378** (1996) 287 [hep-ph/9602277]; *Jet cross sections at next-to-leading order*, *Acta Phys. Polon.* **B28** (1997) 863 [hep-ph/9612236].

[13] M. Dasgupta, L. Magnea and G. Smye, *Universality of $1/Q$ corrections revisited*, *J. High Energy Phys.* **11** (1999) 025 [hep-ph/9911316];
G.E. Smye, *On the $1/Q$ correction to the C-parameter at two loops*, *J. High Energy Phys.* **05** (2001) 005 [hep-ph/0101323].

[14] Z. Nagy and Z. Trocsanyi, *Next-to-leading order calculation of four-jet observables in electron positron annihilation*, *Phys. Rev.* **D 59** (1999) 014020 [hep-ph/9806317].

[15] L. Dixon and A. Signer, *Complete $O(\alpha_s^3)$ results for $e^+e^- \to (\gamma, Z) \to$ four jets*, *Phys. Rev.* **D 56** (1997) 4031 [hep-ph/9706285];
J.M. Campbell, M.A. Cullen and E.W.N. Glover, *Four jet event shapes in electron-positron annihilation*, *Eur. Phys. J.* **C 9** (1999) 245 [hep-ph/9809429];
S. Weinzierl and D.A. Kosower, *QCD corrections to four-jet production and three-jet structure in e^+e^- annihilation*, *Phys. Rev.* **D 60** (1999) 054028 [hep-ph/9901277].

[16] A. Banfi, G.P. Salam and G. Zanderighi, under preparation.

JHEP05(2001)040

[17] G.P. Salam and G. Zanderighi, *Power corrections and the interplay between perturbative and nonperturbative phenomena*, *Nucl. Phys.* **86** *(Proc. Suppl.)* (2000) 430 [hep-ph/9909324].

[18] G.P. Korchemsky and G. Sterman, *Power corrections to event shapes and factorization*, *Nucl. Phys.* **B 555** (1999) 335 [hep-ph/9902341];
G.P. Korchemsky and S. Tafat, *On power corrections to the event shape distributions in QCD*, *J. High Energy Phys.* **10** (2000) 010 [hep-ph/0007005].

[19] V. Antonelli, M. Dasgupta and G.P. Salam, *Resummation of thrust distributions in DIS*, *J. High Energy Phys.* **02** (2000) 001 [hep-ph/9912488].